

IOWA STATE UNIVERSITY

Digital Repository

Materials Science and Engineering Publications

Materials Science and Engineering

2013

Effects of parameter variations on negative effective constitutive parameters of non-metallic metamaterials

Yang Li

Iowa State University

Nicola Bowler

Iowa State University, nbowler@iastate.edu

Follow this and additional works at: http://lib.dr.iastate.edu/mse_pubs

 Part of the [Electrical and Computer Engineering Commons](#), and the [Materials Science and Engineering Commons](#)

The complete bibliographic information for this item can be found at http://lib.dr.iastate.edu/mse_pubs/1. For information on how to cite this item, please visit <http://lib.dr.iastate.edu/howtocite.html>.

This Article is brought to you for free and open access by the Materials Science and Engineering at Digital Repository @ Iowa State University. It has been accepted for inclusion in Materials Science and Engineering Publications by an authorized administrator of Digital Repository @ Iowa State University. For more information, please contact digirep@iastate.edu.

Effects of parameter variations on negative effective constitutive parameters of non-metallic metamaterials

Yang Li and Nicola Bowler

Citation: *J. Appl. Phys.* **113**, 063501 (2013); doi: 10.1063/1.4790714

View online: <http://dx.doi.org/10.1063/1.4790714>

View Table of Contents: <http://jap.aip.org/resource/1/JAPIAU/v113/i6>

Published by the [American Institute of Physics](#).

Additional information on J. Appl. Phys.

Journal Homepage: <http://jap.aip.org/>

Journal Information: http://jap.aip.org/about/about_the_journal

Top downloads: http://jap.aip.org/features/most_downloaded

Information for Authors: <http://jap.aip.org/authors>

ADVERTISEMENT

The advertisement banner for AIP Advances features a green and yellow abstract background with flowing lines. The 'AIP Advances' logo is prominently displayed in the center, with 'AIP' in blue and 'Advances' in green. To the right, a circular seal states 'Now Indexed in Thomson Reuters Databases'. Below the logo, the text 'Explore AIP's open access journal:' is followed by a bulleted list of features.

AIPAdvances

Now Indexed in
Thomson Reuters
Databases

Explore AIP's open access journal:

- Rapid publication
- Article-level metrics
- Post-publication rating and commenting

Effects of parameter variations on negative effective constitutive parameters of non-metallic metamaterials

Yang Li^{1,a)} and Nicola Bowler²

¹*Department of Electrical and Computer Engineering and the Center for Nondestructive Evaluation, Iowa State University, Ames, Iowa 50011, USA*

²*Departments of Materials Science and Engineering, Electrical and Computer Engineering, and the Center for Nondestructive Evaluation, Iowa State University, Ames, Iowa 50011, USA*

(Received 25 November 2012; accepted 24 January 2013; published online 8 February 2013)

Analytical expressions describing the variability of effective constitutive parameters of non-metallic metamaterials, as a function of the constituent geometric and material parameters and their variations, have been developed from the total differential of Clausius-Mossotti expressions (using Mie dipole polarizabilities) for the effective (bulk) constitutive parameters of the metamaterial. In practice, these expressions are important for estimating the performance of a metamaterial with particular variations in the parameters of its constituents that arise during the fabrication process, and can be used to guard against extinction of desired double negative (DNG) behavior. With the derived expressions, the effects of parameter variations on effective constitutive parameters of non-metallic metamaterials have been analyzed for three types of metamaterials: (i) cubic arrays of identical magnetodielectric spheres; (ii) cubic arrays of dielectric spheres with equal radius but two different permittivities; and (iii) cubic arrays of dielectric spheres with equal permittivity but two different radii. These effects are evaluated in terms of the calculated variations in values of the effective constitutive parameters of the metamaterial in the vicinity of the DNG or single negative (SNG) band for particular geometric and material parameters and their variations. Results show that variation in the following parameters impacts DNG bandwidth. Listed in order from greatest to least influence: (i) sphere radius; (ii) sphere permittivity and permeability; (iii) lattice constant of the array; and (iv) the constitutive parameters of the array medium, all impact the width of the achievable DNG band. For particular cases studied here, results also show that the DNG behavior may be extinguished if there are 0.78%, 0.016%, and 0.016% variations in all parameters of metamaterial types (i), (ii), and (iii), respectively, as defined above. For the design of non-metallic metamaterials with inclusions, having arbitrary material parameters, in either periodic or random arrangement, the presented results can give a qualitative guide on the level of fabrication tolerances that should be achieved in order to observe the predicted SNG or DNG behavior experimentally.

© 2013 American Institute of Physics. [<http://dx.doi.org/10.1063/1.4790714>]

I. INTRODUCTION

Metamaterials are artificial composite materials, consisting of sub-wavelength building blocks, which can show anomalous and exotic electromagnetic responses.^{1,2} When the lattice constant is much smaller than the operating wavelength, the composite can be treated macroscopically as a homogeneous medium with effective relative permittivity and permeability, ϵ_r^{eff} and μ_r^{eff} . As the first metamaterials implemented experimentally, metal-based metamaterials have achieved rapid development from microwave to visible frequencies in the last decade.^{1,2} To avoid the drawbacks of metal-based metamaterials, such as conduction loss and anisotropy, composites consisting of non-metallic scatterers embedded in a low permittivity matrix have been proposed to achieve metamaterials.^{3–6} This scheme usually achieves negative effective permittivity at the resonance(s) of the Mie electric dipole scattering coefficient, negative effective permeability at the resonance(s) of the Mie magnetic dipole scattering coefficient, and double negative (DNG) behavior

by overlapping resonances of Mie electric and magnetic dipole scattering coefficients.^{5,7–18} In theory, metamaterials are designed with geometric and electric parameters of the building blocks identical to ideal values. In practice, however, these parameters exhibit variations due to non-ideal, achievable fabrication tolerances, which may extinguish DNG behavior. The purpose of this paper is to present an analytical approach to assessing the effects of those parameter variations on DNG behavior of non-metallic metamaterials.

For metal-based metamaterials, the effect of variation in spacing between the electric ring resonator and the cut wire on the absorbance of an absorbing metamaterial was analyzed using a statistics-based method in Ref. 19. The effects of variations of the geometrical parameters and changes in the background on the invisibility properties of the metamaterial cloak were investigated in Ref. 20. The resonant behaviors of metamaterials with elements disordered from their initially periodic arrangement were studied in Refs. 21 and 22. As for non-metallic metamaterials, the influence of size and permittivity distributions of spherical particles on the DNG characteristics of metamaterial was analyzed in Refs. 23 and 24. Further, the effects of scatterer size

^{a)}Electronic mail: 20002000.leon@gmail.com.

variations on the reflection and transmission properties of a metamaterial were investigated in Ref. 25. None of these works, however, give explicit analytical expressions for the variability of effective constitutive parameters of the metamaterial as a function of the constituent geometric and material parameters and their variations.

This paper develops the Clausius-Mossotti relations (using Mie dipole polarizabilities) for effective constitutive parameters of two types of non-metallic metamaterials: a cubic array of identical magnetodielectric spheres and a cubic array of two different magnetodielectric spheres. Explicit analytical expressions for the variability of effective constitutive parameters as a function of the geometric and material parameters of the spheres, the matrix and their variations are developed from the total differential of the Clausius-Mossotti relations. According to these expressions, the effects of parameter variations on the effective constitutive parameters are analyzed for three types of non-metallic metamaterials: (i) cubic arrays of identical magnetodielectric spheres; (ii) cubic arrays of dielectric spheres with equal radius but two different permittivities; and (iii) cubic arrays of dielectric spheres with equal permittivity but two different radii. Here, the term “magnetodielectric” refers to spheres with relative permittivity and permeability both greater than one, or purely dielectric/magnetic spheres.^{13,26} (Reference 13 contains a considerable number of mostly typographical mistakes which have been corrected in Ref. 27.)

The paper is arranged as follows. Sec. II gives the expressions for variability of effective constitutive parameters of non-metallic metamaterials. The presented expressions are tested in Sec. III for particular cases. Comparisons of the effects of different parameters and of different combinations of parameter variations are presented in Sec. IV. The Appendix gives the analytical expressions for the derivatives of Mie dipole scattering coefficients with respect to different parameters.

II. THEORY

A. Cubic arrays of identical magnetodielectric spheres

Magnetodielectric spheres with relative permittivity ϵ_{r1} , relative permeability μ_{r1} , and radius a are arranged on a cubic lattice with lattice constant d , Fig. 1. The matrix medium has

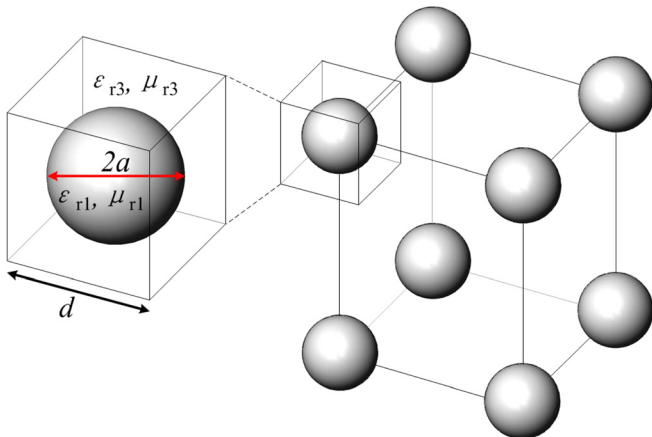


FIG. 1. An array of identical spheres and unit cell geometry.

relative permittivity ϵ_{r3} and relative permeability μ_{r3} (the subscript “3” is chosen so that “2” is reserved for a second type of sphere mentioned later, see Fig. 2 in Sec. II B). When the lattice constant is much smaller than the operating wavelength, $k_0 d$, $\beta d \leq 1$,¹¹ the array can be treated macroscopically as a homogeneous medium with effective relative permittivity ϵ_r^{eff} and effective relative permeability μ_r^{eff} . Here, $k_0 d = \omega \sqrt{\epsilon_0 \mu_0} d$ and $\beta d = \omega \sqrt{\epsilon_r^{\text{eff}} \mu_r^{\text{eff}}} d$. ϵ_r^{eff} can be expressed in the form of Clausius-Mossotti formula [Eq. (3.24) in Ref. 28]

$$\frac{\epsilon_r^{\text{eff}} - \epsilon_{r3}}{\epsilon_r^{\text{eff}} + 2\epsilon_{r3}} = \frac{n\alpha}{3\epsilon_{r3}\epsilon_0}, \quad (1)$$

where ϵ_{r3} is the relative permittivity of the matrix medium, n is the number density of the dipoles, α is the polarisability of each inclusion (sphere), and ϵ_0 is the vacuum permittivity. Multiply \mathbf{E}_0 , which is the local, uniform, electric field exciting a single sphere, on both sides of Eq. (1). Then, replacing the vector quantities by their corresponding scalar ones gives

$$\frac{\epsilon_r^{\text{eff}} - \epsilon_{r3}}{\epsilon_r^{\text{eff}} + 2\epsilon_{r3}} E_0 = \frac{np}{3\epsilon_{r3}\epsilon_0}, \quad (2)$$

where p is the moment of each electric dipole. Solving Eq. (2) for ϵ_r^{eff} gives

$$\epsilon_r^{\text{eff}} = \epsilon_{r3} \frac{2B_j + 3}{3 - B_j} \quad (3)$$

with

$$B_1 = \frac{np}{\epsilon_{r3}\epsilon_0 E_0}, \quad (4)$$

where $j = 1, 2$ depending on the number of types of magnetodielectric spheres composing the array.

Equation (4) can be expressed as¹¹

$$B_1 = -\frac{6\pi i b_1^{\text{sc}}}{(k_0 d)^3 (\epsilon_{r3} \mu_{r3})^{1.5}}, \quad (5)$$

where b_1^{sc} is the Mie electric dipole scattering coefficient given by Eq. (A2), $k_0 d = \omega \sqrt{\epsilon_0 \mu_0} d$ is the electrical lattice

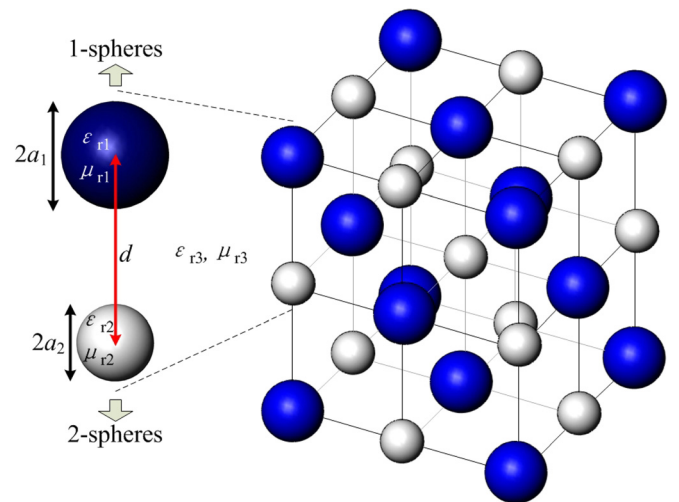


FIG. 2. Two-sphere array and unit cell geometry.

constant. Note that, in contrast with Eq. (76) in Ref. 11, ϵ_r^{eff} in Eq. (3) is relative to the vacuum permittivity ϵ_0 instead of the matrix medium permittivity ϵ_3 . Also note that kd in Eq. (5) is expressed as $k_0\sqrt{\epsilon_{r3}\mu_{r3}}d$ in order to make ϵ_{r3} and μ_{r3} explicit in Eq. (3). By doing so, it becomes easier to study the effects of the variations of ϵ_{r3} and μ_{r3} on ϵ_r^{eff} and μ_r^{eff} .

Expressions for the effective relative permeability μ_r^{eff} can be obtained by replacing ϵ_{r3} and b_1^{sc} in Eqs. (3) and (5), respectively, by μ_{r3} and a_1^{sc} . a_1^{sc} is the Mie magnetic dipole scattering coefficient given by Eq. (A1).

When a metamaterial of the type shown in Fig. 1 is fabricated, departure of ϵ_r^{eff} and μ_r^{eff} from their designed values may arise due to variation in any of the following parameters: k_0a , ϵ_{r1} , μ_{r1} , ϵ_{r3} , μ_{r3} , and k_0d . The electrical dimensions k_0a and k_0d are regarded as parameters here instead of their corresponding physical dimensions to simplify the differentiations. Here, only these six parameters are taken into account to simplify the analysis. In practice, other parameters in addition to those six, such as surface morphology of the spheres, may also affect the designed values of ϵ_r^{eff} and μ_r^{eff} . Based on the definition of the total differential,²⁹ the variability in ϵ_r^{eff} due to its dependent parameters and their variations is given by

$$\Delta\epsilon_r^{\text{eff}} = \sum_m \frac{\partial\epsilon_r^{\text{eff}}}{\partial m} \Delta m, \quad (6)$$

where $m = k_0a, \epsilon_{r1}, \mu_{r1}, \epsilon_{r3}, \mu_{r3}$, and k_0d . Similarly, the expression for $\Delta\mu_r^{\text{eff}}$ can be obtained. Since the derivative may have a negative sign after simple computation, the absolute value of each component variability, $|(\partial\epsilon_r^{\text{eff}}/\partial m)\Delta m|$, is used to describe the worst-case scenario. Note that the definition of the total differential requires that all of the dependent parameters are independent. This requirement is met in many cases, for the following reasons: (i) k_0a and k_0d are the geometric parameters so that they have no correlation with the other four material parameters; (ii) due to the fact that spheres and matrix are fabricated independently, k_0a and k_0d are independent of one another, and ϵ_{r1} and μ_{r1} are independent from ϵ_{r3} and μ_{r3} ; (iii) since there is no functional relation between ϵ_{r1} (ϵ_{r3}) and μ_{r1} (μ_{r3}), their variations are basically due to some random effects, such as a small change in temperature, in the synthesis process. So, ϵ_{r1} (ϵ_{r3}) and μ_{r1} (μ_{r3}) have no correlation with each other. The six parameters are not completely independent, however, especially when approaching large values. For example, the effect of variation in k_0a increases as $(\epsilon_{r1}\mu_{r1})/(\epsilon_{r3}\mu_{r3})$ increases, especially when a/d is large. For this reason, the following analysis is more accurate under circumstances of lower contrast in material properties and lower particle volume fraction. Also note that, according to the definition of the total differential, it is not required that $|\Delta(k_0a)|$, $|\Delta\epsilon_{r1}|$, $|\Delta\mu_{r1}|$, $|\Delta\epsilon_{r3}|$, $|\Delta\mu_{r3}|$, and $|\Delta(k_0d)|$ be small.

In Eq. (6), the derivatives of ϵ_r^{eff} with respect to different parameters are calculated as follows. For $m = k_0a, \epsilon_{r1}, \mu_{r1}, \mu_{r3}$, and k_0d ,

$$\frac{\partial\epsilon_r^{\text{eff}}}{\partial m} = \frac{9\epsilon_{r3}}{(3-B_j)^2} \frac{\partial B_j}{\partial m} \quad (7)$$

with

$$\frac{\partial B_1}{\partial m} = -\frac{6\pi i}{(k_0d)^3(\epsilon_{r3}\mu_{r3})^{1.5}} \frac{\partial b_1^{\text{sc}}}{\partial m} \quad (8)$$

for $m = k_0a, \epsilon_{r1}$, and μ_{r1} ; further

$$\frac{\partial B_1}{\partial \mu_{r3}} = -\frac{6\pi i}{(k_0d)^3(\epsilon_{r3}\mu_{r3})^{1.5}} \left[\frac{\partial b_1^{\text{sc}}}{\partial \mu_{r3}} - 1.5(\mu_{r3})^{-1} b_1^{\text{sc}} \right]; \quad (9)$$

$$\frac{\partial B_1}{\partial(k_0d)} = \frac{18\pi i b_1^{\text{sc}}}{(k_0d)^4(\epsilon_{r3}\mu_{r3})^{1.5}}. \quad (10)$$

And

$$\frac{\partial\epsilon_r^{\text{eff}}}{\partial\epsilon_{r3}} = \frac{2B_j+3}{3-B_j} + \frac{9\epsilon_{r3}}{(3-B_j)^2} \frac{\partial B_j}{\partial\epsilon_{r3}} \quad (11)$$

with

$$\frac{\partial B_1}{\partial\epsilon_{r3}} = -\frac{6\pi i}{(k_0d)^3(\epsilon_{r3}\mu_{r3})^{1.5}} \left[\frac{\partial b_1^{\text{sc}}}{\partial\epsilon_{r3}} - 1.5(\epsilon_{r3})^{-1} b_1^{\text{sc}} \right]. \quad (12)$$

To compute $\Delta\mu_r^{\text{eff}}$, the derivatives of μ_r^{eff} with respect to different parameters are calculated as follows. For $m = k_0a, \epsilon_{r1}, \mu_{r1}, \epsilon_{r3}$, and k_0d ,

$$\frac{\partial\mu_r^{\text{eff}}}{\partial m} = \frac{9\mu_{r3}}{(3-B_j)^2} \frac{\partial B_j}{\partial m} \quad (13)$$

with

$$\frac{\partial B_1}{\partial m} = -\frac{6\pi i}{(k_0d)^3(\epsilon_{r3}\mu_{r3})^{1.5}} \frac{\partial a_1^{\text{sc}}}{\partial m} \quad (14)$$

for $m = k_0a, \epsilon_{r1}$, and μ_{r1} ; further

$$\frac{\partial B_1}{\partial\epsilon_{r3}} = -\frac{6\pi i}{(k_0d)^3(\epsilon_{r3}\mu_{r3})^{1.5}} \left[\frac{\partial a_1^{\text{sc}}}{\partial\epsilon_{r3}} - 1.5(\epsilon_{r3})^{-1} a_1^{\text{sc}} \right]; \quad (15)$$

$$\frac{\partial B_1}{\partial(k_0d)} = \frac{18\pi i a_1^{\text{sc}}}{(k_0d)^4(\epsilon_{r3}\mu_{r3})^{1.5}}. \quad (16)$$

And

$$\frac{\partial\mu_r^{\text{eff}}}{\partial\mu_{r3}} = \frac{2B_j+3}{3-B_j} + \frac{9\mu_{r3}}{(3-B_j)^2} \frac{\partial B_j}{\partial\mu_{r3}} \quad (17)$$

with

$$\frac{\partial B_1}{\partial\mu_{r3}} = -\frac{6\pi i}{(k_0d)^3(\epsilon_{r3}\mu_{r3})^{1.5}} \left[\frac{\partial a_1^{\text{sc}}}{\partial\mu_{r3}} - 1.5(\mu_{r3})^{-1} a_1^{\text{sc}} \right]. \quad (18)$$

In Eqs. (7)–(18), the derivatives of Mie dipole scattering coefficients, a_1^{sc} and b_1^{sc} , with respect to different parameters are given in the Appendix.

B. Cubic arrays of two different magnetodielectric spheres

Two different magnetodielectric spheres are arranged on a cubic lattice with lattice constant $2d$ and matrix medium having relative permittivity ϵ_{r3} , and relative permeability μ_{r3} , Fig. 2. One set of spheres with radius a_1 , and relative permittivity ϵ_{r1} , and relative permeability μ_{r1} will be referred to as the “1-spheres,” and the other set of spheres with radius a_2 , relative permittivity ϵ_{r2} , and relative permeability μ_{r2} will be referred to as the “2-spheres.” Note that the arrangement of the two-sphere array shown in Fig. 2 is one of the seven different arrangements analyzed in Refs. 26 and 30. The Clausius-Mossotti formula gives identical result for different arrangements because it accounts for the number of the electric dipoles of the 1-spheres and 2-spheres per unit cell volume, but not for their relative arrangement. Hence, different arrangements of two-sphere arrays are not taken into account here.

Similar to the case of the cubic arrays of identical magnetodielectric spheres treated in Sec. II A, the two-sphere array can also be treated macroscopically as a homogeneous medium with effective relative permittivity ϵ_r^{eff} and effective relative permeability μ_r^{eff} when the lattice constant is much smaller than the operating wavelength, $k_0d, \beta d \leq 0.5$.^{13,26} The expression for ϵ_r^{eff} in the case of the two-sphere arrays is given by Eq. (3) with $j=2$ and

$$B_2 = -\frac{3\pi i(b_{11}^{\text{sc}} + b_{12}^{\text{sc}})}{(k_0d)^3(\epsilon_{r3}\mu_{r3})^{1.5}}, \quad (19)$$

where b_{11}^{sc} and b_{12}^{sc} are the Mie electric dipole scattering coefficients of the 1-spheres and 2-spheres, respectively, given by Eq. (A2). A similar expression for μ_r^{eff} of two-sphere arrays can be obtained by replacing ϵ_{r3} and b_{li}^{sc} ($i=1, 2$) in Eqs. (3) and (19) by μ_{r3} and a_{li}^{sc} ($i=1, 2$), respectively. a_{li}^{sc} is the Mie magnetic dipole scattering coefficient given by Eq. (A1).

The variability of ϵ_r^{eff} and μ_r^{eff} is a function of the following parameters and their variations: $k_0a_1, k_0a_2, \epsilon_{r1}, \mu_{r1}, \epsilon_{r2}, \mu_{r2}, \epsilon_{r3}, \mu_{r3}$, and k_0d . Here, only these nine parameters are taken into account to simplify the analysis. Similar to the case of the arrays of identical spheres, these parameters are independent in many cases. Due to the increased complexity of the system, the expression for $\Delta\epsilon_r^{\text{eff}}$ in the case of the two-sphere arrays, obtained by total differential of the Clausius-Mossotti relations as described above, contains more terms than in the case of arrays of identical spheres. Referring to Eq. (6), now $m = k_0a_1, k_0a_2, \epsilon_{r1}, \mu_{r1}, \epsilon_{r2}, \mu_{r2}, \epsilon_{r3}, \mu_{r3}$, and k_0d . The expression for $\Delta\mu_r^{\text{eff}}$ in the case of the two-sphere arrays can be obtained in a similar way.

The derivatives of ϵ_r^{eff} with respect to different parameters are computed as follows. For $m = k_0a_1, k_0a_2, \epsilon_{r1}, \mu_{r1}, \epsilon_{r2}, \mu_{r2}, \mu_{r3}$, and k_0d , $\partial\epsilon_r^{\text{eff}}/\partial m$ can be obtained by Eq. (7) with

$$\frac{\partial B_2}{\partial m} = -\frac{3\pi i}{(k_0d)^3(\epsilon_{r3}\mu_{r3})^{1.5}} \frac{\partial b_{11}^{\text{sc}}}{\partial m} \quad (20)$$

for $m = k_0a_1, \epsilon_{r1}, \mu_{r1}$;

$$\frac{\partial B_2}{\partial m} = -\frac{3\pi i}{(k_0d)^3(\epsilon_{r3}\mu_{r3})^{1.5}} \frac{\partial b_{12}^{\text{sc}}}{\partial m} \quad (21)$$

for $m = k_0a_2, \epsilon_{r2}, \mu_{r2}$; further

$$\frac{\partial B_2}{\partial \mu_{r3}} = -\frac{3\pi i}{(k_0d)^3(\epsilon_{r3}\mu_{r3})^{1.5}} \times \left[\left(\frac{\partial b_{11}^{\text{sc}}}{\partial \mu_{r3}} + \frac{\partial b_{12}^{\text{sc}}}{\partial \mu_{r3}} \right) - 1.5(\mu_{r3})^{-1}(b_{11}^{\text{sc}} + b_{12}^{\text{sc}}) \right]; \quad (22)$$

$$\frac{\partial B_2}{\partial(k_0d)} = \frac{9\pi i(b_{11}^{\text{sc}} + b_{12}^{\text{sc}})}{(k_0d)^4(\epsilon_{r3}\mu_{r3})^{1.5}}. \quad (23)$$

$\partial\epsilon_r^{\text{eff}}/\partial\epsilon_{r3}$ can be expressed as Eq. (11) with

$$\frac{\partial B_2}{\partial \epsilon_{r3}} = -\frac{3\pi i}{(k_0d)^3(\epsilon_{r3}\mu_{r3})^{1.5}} \times \left[\left(\frac{\partial b_{11}^{\text{sc}}}{\partial \epsilon_{r3}} + \frac{\partial b_{12}^{\text{sc}}}{\partial \epsilon_{r3}} \right) - 1.5(\epsilon_{r3})^{-1}(b_{11}^{\text{sc}} + b_{12}^{\text{sc}}) \right]. \quad (24)$$

The derivatives of μ_r^{eff} with respect to different parameters are calculated as follows. For $m = k_0a_1, k_0a_2, \epsilon_{r1}, \mu_{r1}, \epsilon_{r2}, \mu_{r2}, \epsilon_{r3}$, and k_0d , $\partial\mu_r^{\text{eff}}/\partial m$ can be obtained by Eq. (13) with

$$\frac{\partial B_2}{\partial m} = -\frac{3\pi i}{(k_0d)^3(\epsilon_{r3}\mu_{r3})^{1.5}} \frac{\partial a_{11}^{\text{sc}}}{\partial m} \quad (25)$$

for $m = k_0a_1, \epsilon_{r1}$, and μ_{r1} ;

$$\frac{\partial B_2}{\partial m} = -\frac{3\pi i}{(k_0d)^3(\epsilon_{r3}\mu_{r3})^{1.5}} \frac{\partial a_{12}^{\text{sc}}}{\partial m} \quad (26)$$

for $m = k_0a_2, \epsilon_{r2}$, and μ_{r2} ; further

$$\frac{\partial B_2}{\partial \epsilon_{r3}} = -\frac{3\pi i}{(k_0d)^3(\epsilon_{r3}\mu_{r3})^{1.5}} \times \left[\left(\frac{\partial a_{11}^{\text{sc}}}{\partial \epsilon_{r3}} + \frac{\partial a_{12}^{\text{sc}}}{\partial \epsilon_{r3}} \right) - 1.5(\epsilon_{r3})^{-1}(a_{11}^{\text{sc}} + a_{12}^{\text{sc}}) \right]; \quad (27)$$

$$\frac{\partial B_2}{\partial(k_0d)} = \frac{9\pi i(a_{11}^{\text{sc}} + a_{12}^{\text{sc}})}{(k_0d)^4(\epsilon_{r3}\mu_{r3})^{1.5}}. \quad (28)$$

$\partial\mu_r^{\text{eff}}/\partial\mu_{r3}$ can be expressed as Eq. (17) with

$$\frac{\partial B_2}{\partial \mu_{r3}} = -\frac{3\pi i}{(k_0d)^3(\epsilon_{r3}\mu_{r3})^{1.5}} \times \left[\left(\frac{\partial a_{11}^{\text{sc}}}{\partial \mu_{r3}} + \frac{\partial a_{12}^{\text{sc}}}{\partial \mu_{r3}} \right) - 1.5(\mu_{r3})^{-1}(a_{11}^{\text{sc}} + a_{12}^{\text{sc}}) \right]. \quad (29)$$

The derivatives of Mie dipole scattering coefficients $a_{11}^{\text{sc}}, a_{12}^{\text{sc}}, b_{11}^{\text{sc}}$, and b_{12}^{sc} with respect to various parameters are given in the Appendix.

III. VERIFICATION

In this section and Sec. IV, magnetodielectric spheres in all the cases considered are lossless. In general, the effective

constitutive parameters of a composite may be complex even if the constituents are lossless.^{31–34} For the cases under study, non-metallic metamaterials consisting of cubic arrays of lossless magnetodielectric spheres, the effective constitutive parameters are real away from the resonance regions, and are complex in the resonance regions corresponding to bandgaps in the dispersion diagram.^{3,11,13} However, the focus of this work is on the lossless traveling waves (with real wavenumber β) that can be supported by the array. Hence, in all the cases under study, only the real parts of the effective constitutive parameters calculated by the Clausius-Mossotti expressions are considered. In the region of homogenization, k_0d , $\beta d \leq 1$ (k_0d , $\beta d \leq 0.5$) for arrays of identical spheres (two-sphere arrays), the real parts of the effective constitutive parameters calculated here by Clausius-Mossotti expressions, Eq. (3), are in good consistency with those, which are real values, computed by Shore-Yaghjian formulas.¹¹ Further, only the real part of each partial derivative of an effective constitutive parameter with respect to a parameter in Eq. (6) is considered so as to give a real variability of effective constitutive parameters, eventually.

A. Clausius-Mossotti formulas

First, the Clausius-Mossotti expressions for the effective constitutive parameters of non-metallic metamaterials consisting of an array of identical spheres, Eqs. (3) and (5), and an array of two types of spheres, Eqs. (3) and (19), are tested by comparing the dispersion diagrams obtained by the following relation:¹¹

$$\frac{\beta d}{k_0d} = \sqrt{\epsilon_r^{\text{eff}} \mu_r^{\text{eff}}}, \quad (30)$$

with those calculated by MIT photonic-bands (MPB).³⁵ MPB computes fully vectorial eigenmodes of Maxwell's equations with periodic boundary conditions by preconditioned conjugate-gradient minimization of the block Rayleigh quotient in a plane-wave basis.³⁵ Since MPB can only treat dielectric periodic structures, arrays considered in this section are all of dielectric spheres. Fig. 3 shows the

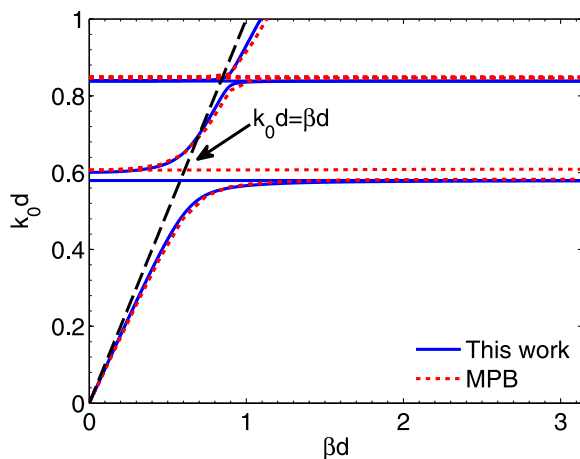


FIG. 3. Comparison of dispersion diagrams for an array of identical spheres, Fig. 1, obtained by formulas presented here, Eqs. (3), (5), and (30), with that calculated by MPB.³⁵ The 25 lowest bands computed by MPB are shown. In this calculation, $\epsilon_{r1} = 400$, $\mu_{r1} = \epsilon_{r3} = \mu_{r3} = 1$, and $a/d = 0.2672$.

dispersion diagram for an array of identical dielectric spheres whose parameters are chosen to match those of the larger sphere considered in a design example given in Refs. 23 and 36. The parameter values are provided in the figure caption. This array does not support backward wave propagation but, nonetheless, it can be used to test the effectiveness of the presented Clausius-Mossotti formula. The two-sphere array of Fig. 4 is a design example in Refs. 23 and 36, which shows backward wave propagation in the vicinity of $k_0d = 0.8386$. As shown in Figs. 3 and 4, good agreement is achieved between the calculations of MPB and the formulae presented herein, for these cases. Note that the MPB result for the two-sphere array, Fig. 4, is shown only in the range $0 < \beta d < \pi/2$, instead of $0 < \beta d < \pi$, because, in MPB, the lattice constant of this two-sphere array is set to be twice the separation of adjacent spheres, i.e., $d' = 2d$, to guarantee the translational symmetry in the x , y , and z directions. This means that the size of the corresponding reciprocal lattice in the Brillouin zone is halved.³⁷

B. Expressions for the variabilities of effective constitutive parameters

Next, the variabilities of effective constitutive parameters of non-metallic metamaterials consisting of an array of identical spheres and of a two-sphere array, Eq. (6), are tested. In this section, the non-metallic metamaterials are designed following the design procedure in Ref. 38 to achieve a DNG behavior in the vicinity of $k_0d = 0.4$, which meets the homogenization criteria of metamaterials consisting of an array of identical spheres, k_0d , $\beta d \leq 1$, and of a two-sphere array, k_0d , $\beta d \leq 0.5$. $\Delta\epsilon_r^{\text{eff}}$ and $\Delta\mu_r^{\text{eff}}$ of an array of identical spheres, Fig. 5, are computed by Eq. (6) and compared with those calculated by expressions developed by Mathematica. Good agreement is achieved. Using Mathematica, the derivatives of ϵ_r^{eff} and μ_r^{eff} in Eq. (6) are obtained by differentiating Eq. (3) with respect to k_0a , ϵ_{r1} , μ_{r1} , ϵ_{r3} , μ_{r3} , and k_0d . Note that the expressions developed by Mathematica are much more cumbersome than the presented ones.

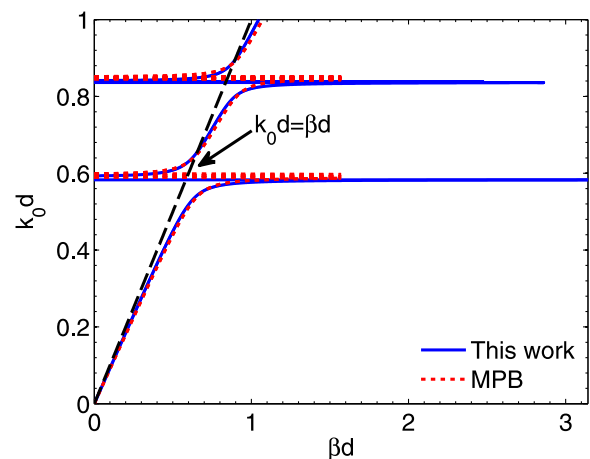


FIG. 4. Comparison of dispersion diagrams for a two-sphere array, Fig. 2, obtained by formulas presented here, Eqs. (3), (19), and (30), with that calculated by MPB.³⁵ The 60 lowest bands computed by MPB are shown. In this calculation, $\epsilon_{r1} = \epsilon_{r2} = 400$, $\mu_{r1} = \mu_{r2} = \epsilon_{r3} = \mu_{r3} = 1$, $a_1/d = 0.187$, and $a_2/d = 0.2672$.

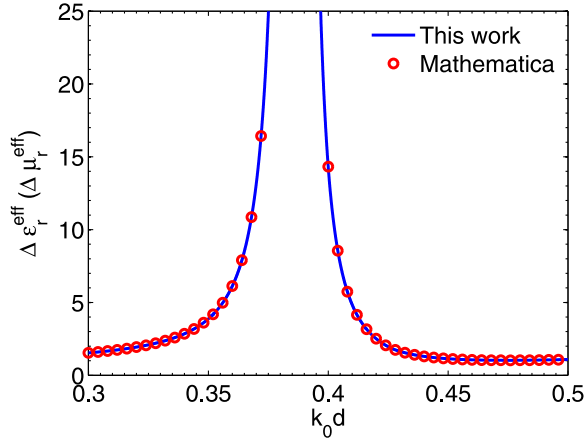


FIG. 5. Comparison of variabilities of effective constitutive parameters in the vicinity of the DNG band ($k_0d = 0.4$) of a metamaterial consisting of an array of identical spheres, Fig. 1, computed by the formula presented herein Eq. (6), with those calculated by expressions developed by Mathematica. In this calculation, $\epsilon_{r1} = \mu_{r1} = 23.9$, $\epsilon_{r3} = \mu_{r3} = 1$, and $a/d = 0.45$; $\Delta m/m = 5\%$ with $m = k_0a$, ϵ_{r1} , μ_{r1} , ϵ_{r3} , μ_{r3} , and k_0d .

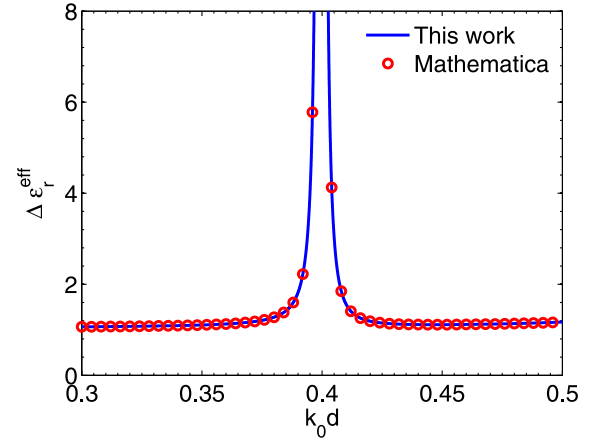
Further, $\Delta\epsilon_r^{\text{eff}}$ and $\Delta\mu_r^{\text{eff}}$ of a two-sphere array, Fig. 6, are computed by Eq. (6) and compared with those calculated by expressions developed by Mathematica. Again, good agreement is achieved.

IV. RESULTS

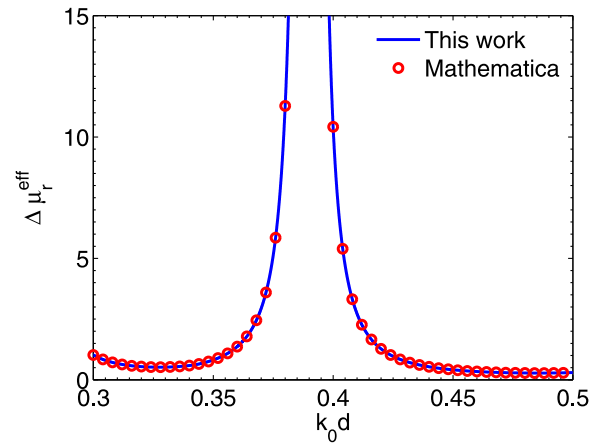
In this section, the effects of parameter variations on the effective constitutive parameters are analyzed for three types of non-metallic metamaterials: (i) a cubic array of identical magnetodielectric spheres; (ii) a cubic array of two types of dielectric spheres with equal radius but different permittivities; and (iii) a similar array of two types of dielectric spheres with equal permittivity but different radii. For each of these, the effect of variation in individual parameters is first compared. Then, the effects of different combinations of parameter variations are analyzed. The two metamaterials studied in Sec. III B are used as the reference cases in Secs. IV A and IV B, respectively.

A. Cubic arrays of identical magnetodielectric spheres

Utilizing Eq. (6), $\Delta\epsilon_r^{\text{eff}}$ is calculated as one of k_0a , ϵ_{r1} , μ_{r1} , ϵ_{r3} , μ_{r3} , and k_0d varies by 5% from its nominal value, Table I. As shown in Fig. 7, variation of k_0a has the most significant effect on $\Delta\epsilon_r^{\text{eff}}$; variation of k_0d has the second most significant effect on $\Delta\epsilon_r^{\text{eff}}$ over the lower part of the DNG band studied ($k_0d \leq 0.4$) and the fourth most significant effect over the higher part of the DNG band studied ($k_0d \geq 0.4$); variations of ϵ_{r1} and μ_{r1} have similar effects on $\Delta\epsilon_r^{\text{eff}}$, giving rise to the third most significant effects on $\Delta\epsilon_r^{\text{eff}}$ over the lower part of the DNG band studied ($k_0d \leq 0.4$) and the second most significant effects over the higher part of the DNG band studied ($k_0d \geq 0.4$); whereas variations of ϵ_{r3} and μ_{r3} have the least effects on $\Delta\epsilon_r^{\text{eff}}$. Hence, it is noted that variation in the parameters of the sphere (sphere radius, permittivity, and permeability) perturbs the predicted behavior of the DNG band more strongly than other parameters of the system. Note that effects of the variations in k_0a and k_0d on



(a)



(b)

FIG. 6. Comparisons of variabilities of effective relative permittivity (a), and permeability (b), in the vicinity of the DNG band ($k_0d = 0.4$) of a metamaterial consisting of a two-sphere array, Fig. 2, computed by the formula presented herein Eq. (6), with those calculated by expressions developed by Mathematica. In this calculation, $\epsilon_{r1} = 621.1$, $\epsilon_{r2} = 302.7$, $\mu_{r1} = \mu_{r2} = \epsilon_{r3} = \mu_{r3} = 1$, and $a_1/d = a_2/d = 0.45$; $\Delta m/m = 5\%$ with $m = k_0a_1$, ϵ_{r1} , μ_{r1} , k_0a_2 , ϵ_{r2} , μ_{r2} , ϵ_{r3} , μ_{r3} , and k_0d .

$\Delta\epsilon_r^{\text{eff}}$ are exactly the same as those on $\Delta\mu_r^{\text{eff}}$ since both negative ϵ_r^{eff} and negative μ_r^{eff} in the vicinity of the DNG band are provided by the same magnetodielectric sphere embedded in a simple cubic lattice, which has only one set of geometric parameters: k_0a and k_0d .

In practical fabrication, it is expected that a metamaterial consisting of an array of identical spheres would exhibit a combination of variations in its parameters, due to achievable fabrication tolerances. To analyze the effects of different combinations of parameter variations on effective constitutive parameters of the metamaterial in the vicinity of the DNG band, the following parameter variations are studied, $\Delta m/m = 0.78\%$, 3% , and 5% ($m = k_0a$, ϵ_{r1} , μ_{r1} , ϵ_{r3} , μ_{r3} , and k_0d), where variation of the six parameters is assumed to

TABLE I. The parameter with 5% variation (while others have no variation) in each calculation of variability of effective constitutive parameters of a non-metallic metamaterial consisting of an array of identical spheres, Fig. 1.

| Calculation | I | II | III | IV | V | VI |
|-------------|--------|-----------------|------------|-----------------|------------|--------|
| Parameter | k_0a | ϵ_{r1} | μ_{r1} | ϵ_{r3} | μ_{r3} | k_0d |

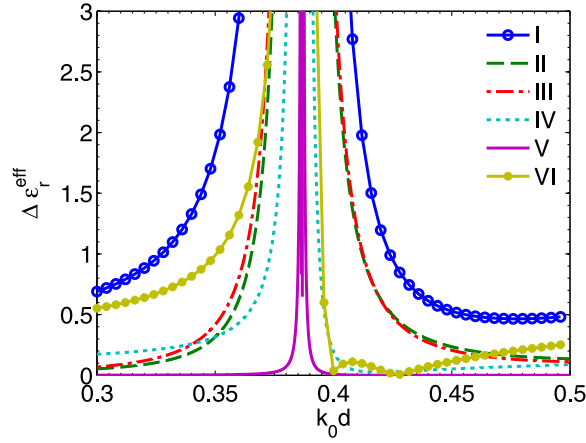


FIG. 7. Variabilities of effective relative permittivity in the vicinity of the DNG band ($k_0d = 0.4$) of a non-metallic metamaterial consisting of a cubic array of identical magnetodielectric spheres, Fig. 1, in each calculation, Table I. Parameters of this array are as in Fig. 5. The equivalent plot for $\Delta\mu_r^{\text{eff}}$ is not shown here since the only difference is that the effects of variations in ϵ_{r1} , ϵ_{r3} and those of variations in μ_{r1} , μ_{r3} are interchanged.

be equal to each other. For each of these combinations, $\Delta\epsilon_r^{\text{eff}}$ is calculated from Eq. (6). The ideal value of effective relative permittivity, $\epsilon_r^{\text{eff,idl}}$, is computed from Eq. (3). Based on these results, the variation range of ϵ_r^{eff} ,

$$\epsilon_r^{\text{eff,idl}} - \Delta\epsilon_r^{\text{eff}} < \epsilon_r^{\text{eff}} < \epsilon_r^{\text{eff,idl}} + \Delta\epsilon_r^{\text{eff}}, \quad (31)$$

is obtained for each of these combinations, giving the shaded areas in Fig. 8. Similarly, the variation range of μ_r^{eff} can be obtained. It can be seen that the variation ranges increase as the parameter variations increase. According to these results, it is seen that the DNG behavior may be extinguished when $\Delta m/m \geq 0.78\%$ ($m = k_0a$, ϵ_{r1} , μ_{r1} , ϵ_{r3} , μ_{r3} , and k_0d).

B. Cubic arrays of dielectric spheres with equal radius but two different permittivities

In this section, a similar analysis to that described in Sec. IV A is performed for an array of two types of dielectric spheres, with equal radius but different permittivities,

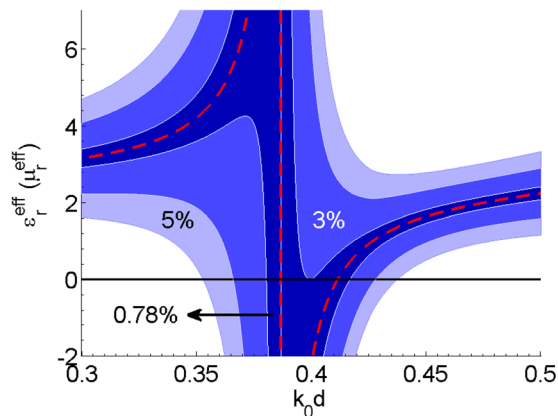


FIG. 8. Ideal values and variation ranges of the effective relative permittivity and permeability for a non-metallic metamaterial consisting of a cubic array of identical magnetodielectric spheres, Fig. 1. Dashed line: ideal values of ϵ_r^{eff} and μ_r^{eff} ; dark, medium, and light shaded areas: variation ranges for $\Delta m/m = 0.78\%$, 3% , and 5% with $m = k_0a$, ϵ_{r1} , μ_{r1} , ϵ_{r3} , μ_{r3} , and k_0d . Other parameters are as in Fig. 5.

TABLE II. The parameter with 5% variation (while others have no variation) in each calculation of variabilities of effective constitutive parameters of a non-metallic metamaterial consisting of a two-sphere array, Fig. 2.

| Calculation | I | II | III | IV | V | VI | VII | VIII | IX |
|-------------|----------|-----------------|------------|----------|-----------------|------------|-----------------|------------|--------|
| Parameter | k_0a_1 | ϵ_{r1} | μ_{r1} | k_0a_2 | ϵ_{r2} | μ_{r2} | ϵ_{r3} | μ_{r3} | k_0d |

arranged on the nodes of a simple-cubic lattice, Fig. 2. As before, the variability of effective constitutive parameters of the non-metallic metamaterial is computed by Eq. (6). In each computation, one of k_0a_1 , ϵ_{r1} , μ_{r1} , k_0a_2 , ϵ_{r2} , μ_{r2} , ϵ_{r3} , μ_{r3} , and k_0d is set to be 5% different from the nominal value while other parameters have no variation, Table II. The calculated $\Delta\epsilon_r^{\text{eff}}$ and $\Delta\mu_r^{\text{eff}}$ are shown in Fig. 9. Since the negative ϵ_r^{eff} (μ_r^{eff}) is provided by the first resonance of Mie electric (magnetic) dipole scattering coefficient of the 1-spheres (2-spheres), their parameter variations, Δk_0a_1 , $\Delta\epsilon_{r1}$, and $\Delta\mu_{r1}$ (Δk_0a_2 , $\Delta\epsilon_{r2}$, and $\Delta\mu_{r2}$), have the dominant effects on ϵ_r^{eff} (μ_r^{eff}) in the vicinity of the DNG band. Hence, only the effects of parameter variations of 1-spheres (2-spheres) on ϵ_r^{eff} (μ_r^{eff}) are shown in Fig. 9 and are analyzed in detail. As shown in Fig. 9(a): variation of

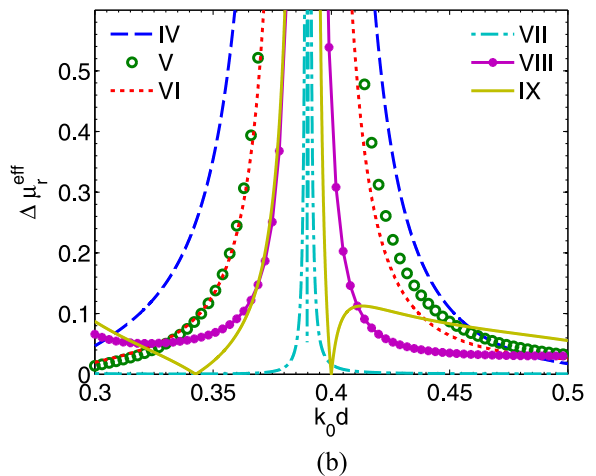
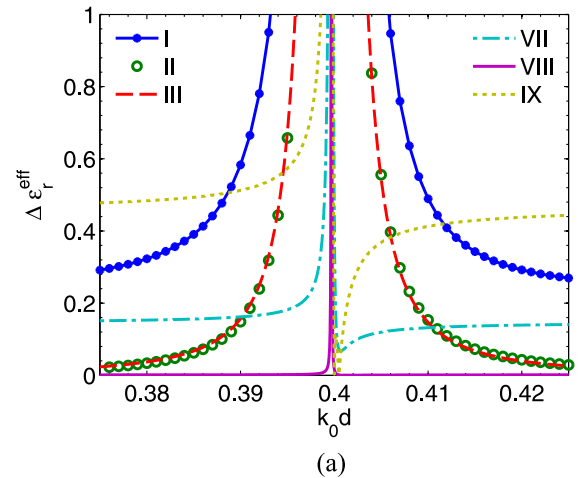


FIG. 9. Variabilities of effective relative permittivity (a), and permeability (b), in the vicinity of the DNG band ($k_0d = 0.4$) of a non-metallic metamaterial consisting of a cubic array of dielectric spheres with equal radius but two different permittivities, Fig. 2, in each calculation, Table II. Parameters of this array are as in Fig. 6.

$k_0 a_1$ has the most significant effect on $\Delta \epsilon_r^{\text{eff}}$; variations of ϵ_{r1} and μ_{r1} have similar effects on $\Delta \epsilon_r^{\text{eff}}$, which are less than that of $k_0 a_1$; variation of $k_0 d$ has the fourth most significant effect on $\Delta \epsilon_r^{\text{eff}}$; and variations of ϵ_{r3} and μ_{r3} have the least effects on $\Delta \epsilon_r^{\text{eff}}$. As shown in Fig. 9(b): variation of $k_0 a_2$ has the most significant effect on $\Delta \mu_r^{\text{eff}}$; variations of ϵ_{r2} and μ_{r2} have similar effects on $\Delta \mu_r^{\text{eff}}$, which are less than that of $k_0 a_2$; variations of μ_{r3} and $k_0 d$ have similar effects on $\Delta \mu_r^{\text{eff}}$, which are less than those of ϵ_{r2} and μ_{r2} ; and variation of ϵ_{r3} has the least effect on $\Delta \epsilon_r^{\text{eff}}$.

To analyze the effects of different combinations of parameter variations on ϵ_r^{eff} (μ_r^{eff}) in the vicinity of the DNG band, the following parameter variations are studied, $\Delta m/m = 0.016\%$, 0.03% , and 0.1% (1.2% , 3% , and 5%) with $m = k_0 a_1, \epsilon_{r1}, \mu_{r1}, k_0 a_2, \epsilon_{r2}, \mu_{r2}, \epsilon_{r3}, \mu_{r3}$, and $k_0 d$, are taken into account. In each case, variations of the nine parameters are assumed equal to each other. For each of these combinations, the variation range of ϵ_r^{eff} , Eq. (31), is obtained, giving the shaded areas in Fig. 10. Similarly, the variation range of μ_r^{eff} can be obtained. It can be seen that the variation ranges increase as the parameter variations increase. The negative

ϵ_r^{eff} (μ_r^{eff}) may be extinguished when $\Delta m/m \geq 0.016\%$ (1.2%) with $m = k_0 a_1, \epsilon_{r1}, \mu_{r1}, k_0 a_2, \epsilon_{r2}, \mu_{r2}, \epsilon_{r3}, \mu_{r3}$, and $k_0 d$. Consequently, the DNG behavior may be extinguished when $\Delta m/m \geq 0.016\%$. Note that the negative ϵ_r^{eff} of this metamaterial is much more sensitive to parameter variations than negative μ_r^{eff} . The reason for this is that the first resonance of the Mie electric dipole scattering coefficient of the set of 1-spheres for which, in this calculation, $\epsilon_{r1} = 621.1$ and which provides the negative ϵ_r^{eff} , is narrower than the first resonance of the Mie magnetic dipole scattering coefficient of the set of 2-spheres ($\epsilon_{r2} = 302.7$), which provides the negative μ_r^{eff} .

C. Cubic arrays of dielectric spheres with equal permittivity but two different radii

Following the design procedure presented in Ref. 38, a non-metallic metamaterial consisting of a cubic array of two types of dielectric spheres with equal permittivity but different radii is designed with parameters $\epsilon_{r1} = \epsilon_{r2} = 621.1$, $\mu_{r1} = \mu_{r2} = \epsilon_{r3} = \mu_{r3} = 1$, $a_1/d = 0.45$, and $a_2/d = 0.31$, to yield DNG behavior in the vicinity of $k_0 d = 0.4$, similar to

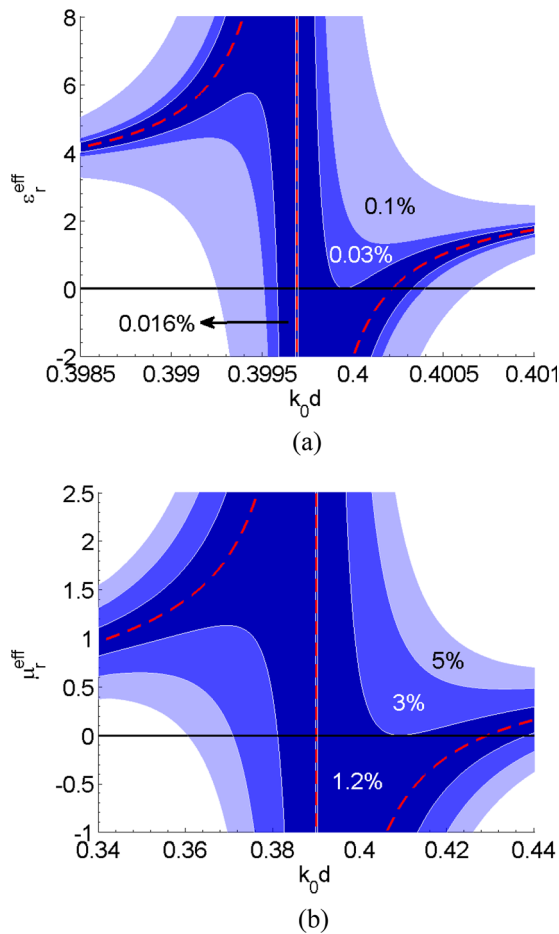


FIG. 10. Ideal values and variation ranges of the effective relative permittivity (a), and permeability (b), for a non-metallic metamaterial consisting of a cubic array of dielectric spheres with equal radius but two different permittivities, Fig. 2, with six combinations of parameter variations. Dashed line: ideal values of ϵ_r^{eff} (a), and μ_r^{eff} (b); dark, medium, and light shaded areas: variation ranges for $\Delta m/m = 0.016\%$, 0.03% , and 0.1% (a), 1.2% , 3% , and 5% (b) with $m = k_0 a_1, \epsilon_{r1}, \mu_{r1}, k_0 a_2, \epsilon_{r2}, \mu_{r2}, \epsilon_{r3}, \mu_{r3}$, and $k_0 d$. Other parameters are as in Fig. 6.

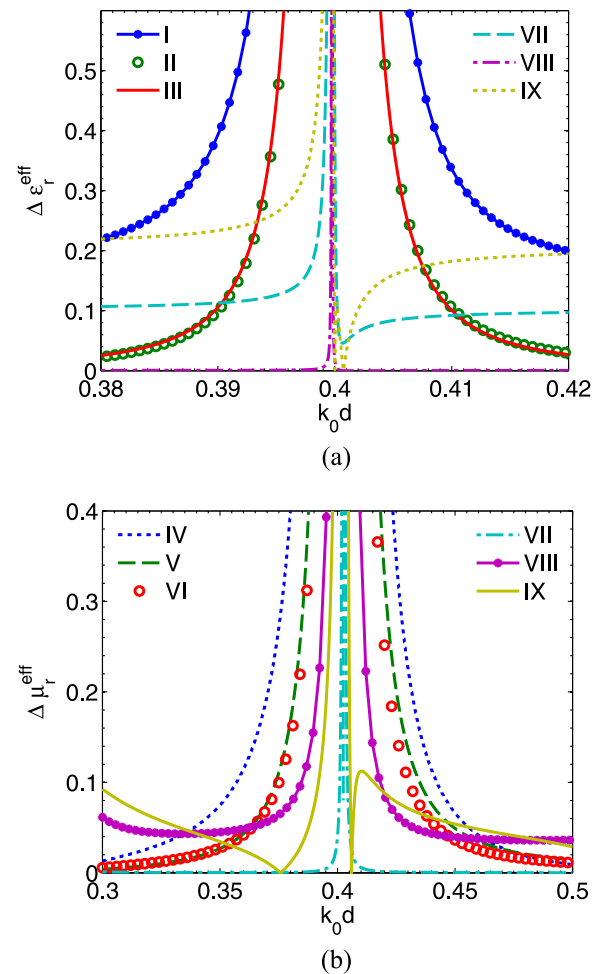


FIG. 11. Variabilities of effective relative permittivity (a), and permeability (b), in the vicinity of the DNG band ($k_0 d = 0.4$) of a non-metallic metamaterial consisting of a cubic array of dielectric spheres with equal permittivity but two different radii, Fig. 2, in each calculation, Table II. In these calculations, $\epsilon_{r1} = \epsilon_{r2} = 621.1$, $\mu_{r1} = \mu_{r2} = \epsilon_{r3} = \mu_{r3} = 1$, $a_1/d = 0.45$, and $a_2/d = 0.31$.

the behavior of the metamaterials analyzed in Secs. IV A and IV B.

Similar to the analysis in the first paragraph of Sec. IV B, the effects of different parameters are compared for this metamaterial. As shown in Fig. 11(a): variation of k_0a_1 has the most significant effect on $\Delta\epsilon_r^{\text{eff}}$; variations of ϵ_{r1} and μ_{r1} have similar effects on $\Delta\epsilon_r^{\text{eff}}$, which are less than that of k_0a_1 ; variation of k_0d has the fourth most significant effect on $\Delta\epsilon_r^{\text{eff}}$; and variations of ϵ_{r3} and μ_{r3} have the least effects on $\Delta\epsilon_r^{\text{eff}}$. As shown in Fig. 11(b): variation of k_0a_2 has the most significant effect on $\Delta\mu_r^{\text{eff}}$; variations of ϵ_{r2} and μ_{r2} have similar effects on $\Delta\mu_r^{\text{eff}}$, which are less than that of k_0a_2 ; variation of μ_{r3} has the fourth most significant effect on $\Delta\mu_r^{\text{eff}}$; and variations of ϵ_{r3} and k_0d have the least effects on $\Delta\mu_r^{\text{eff}}$.

Similar to the analysis in the second paragraph of Sec. IV B, the effects of different combinations of parameter variations on ϵ_r^{eff} and μ_r^{eff} in the vicinity of the DNG band are investigated for this metamaterial. As shown in Fig. 12, the variation ranges increase as the parameter variations increase. The negative ϵ_r^{eff} (μ_r^{eff}) may be extinguished when $\Delta m/m \geq 0.016\%$ (0.4%) with $m = k_0a_1, \epsilon_{r1}, \mu_{r1}, k_0a_2$,

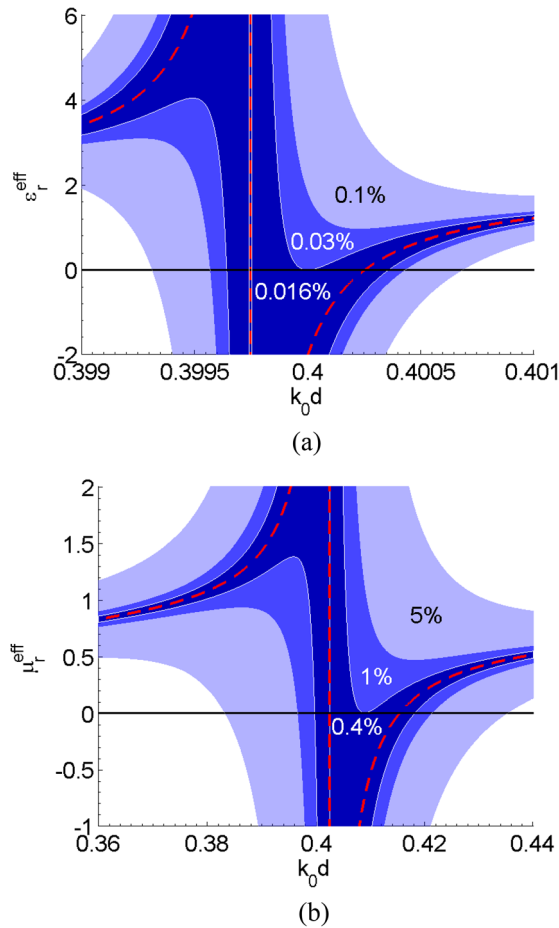


FIG. 12. Ideal values and variation ranges of the effective relative permittivity (a), and permeability (b), for a non-metallic metamaterial consisting of a cubic array of dielectric spheres with equal permittivity but two different radii, Fig. 2, with six combinations of parameter variations. Dashed line: ideal values of ϵ_r^{eff} (a), and μ_r^{eff} (b); dark, medium, and light shaded areas: variation ranges for $\Delta m/m = 0.016\%$, 0.03% , and 0.1% (a), 0.4% , 1% , and 5% (b) with $m = k_0a_1, \epsilon_{r1}, \mu_{r1}, k_0a_2, \epsilon_{r2}, \mu_{r2}, \epsilon_{r3}, \mu_{r3}$, and k_0d . Other parameters are as in Fig. 11.

$\epsilon_{r2}, \mu_{r2}, \epsilon_{r3}, \mu_{r3}$, and k_0d . Hence, the DNG behavior may be extinguished when $\Delta m/m \geq 0.016\%$. Note that the negative ϵ_r^{eff} of this metamaterial is more sensitive to parameter variations than negative μ_r^{eff} . The reason is that the first resonance of Mie electric dipole scattering coefficient, which corresponds to 1-spheres ($a_1/d = 0.45$) and provides negative ϵ_r^{eff} , is narrower than the first resonance of Mie magnetic dipole scattering coefficient, which corresponds to 2-spheres ($a_2/d = 0.31$) and provides negative μ_r^{eff} .

V. CONCLUSION

Considering constitutive parameters of the array medium, the Clausius-Mossotti relations (using Mie dipole polarizabilities) have been developed for calculating the effective (bulk) constitutive parameters of two types of non-metallic metamaterials: a cubic array of identical magnetodielectric spheres and a cubic array of two different dielectric spheres. These relations have been tested by comparing their dispersion diagrams with those calculated by MPB. Analytical expressions describing the variability of effective constitutive parameters of non-metallic metamaterials, as a function of the constituent geometric and material parameters and their variations, have been developed from the total differential of the derived Clausius-Mossotti relations. These expressions have been verified by comparing their results with those calculated by analytical expressions developed by Mathematica. In practical fabrication, the presented analysis is important for predicting the performance of a metamaterial with particular variations in the parameters of its constituents, which arise due to achievable tolerance in the fabrication process, and can be used to guard against extinction of desired DNG behavior. Based on this theory, the effects of different parameters and of different combinations of parameter variations on effective constitutive parameters have been analyzed for three types of metamaterials: (i) cubic arrays of identical magnetodielectric spheres; (ii) cubic arrays of dielectric spheres with equal radius but two different permittivities; and (iii) cubic arrays of dielectric spheres with equal permittivity but two different radii. These effects are evaluated in terms of the computed variations in values of the effective constitutive parameters of the metamaterial in the vicinity of the DNG or single negative (SNG) band for particular geometric and material parameters and their variations. Results show that variation in the following parameters impacts DNG bandwidth. In order from most to least: (i) sphere radius; (ii) sphere permittivity and permeability; (iii) lattice constant of the array, and (iv) the constitutive parameters of the array medium, all impact the width of the achievable DNG band. For particular cases studied here, results also show that the DNG behavior may be extinguished if there are 0.78%, 0.016%, and 0.016% variations in all parameters of metamaterial types (i), (ii), and (iii), respectively, as defined above. For the design of non-metallic metamaterials with inclusions, having arbitrary material parameters, in either periodic or random arrangement, the presented results can give a qualitative guide on the level of fabrication tolerances that should be achieved in order to observe SNG or DNG behavior experimentally. The extinction of DNG

behavior at variances above an extremely tight fabrication tolerance (0.016%) in all the geometric and material parameters of the particular cases considered here suggests that fabrication of metamaterial types (ii) and (iii) may not be realizable in practice.

ACKNOWLEDGMENTS

This material is based upon work supported by the Air Force Research Laboratory under Contract No. FA8650-04-C-5228 at Iowa State University's Center for NDE. The authors wish to express their deep gratitude to Dr. Robert A. Shore (Air Force Research Laboratory, Hanscom AFB, MA) and Mr. Xing-Xiang Liu (The University of Texas at Austin) for very helpful discussions and communications.

APPENDIX: ANALYTICAL EXPRESSIONS FOR MIE DERIVATIVES

In this appendix, analytical expressions are developed for the derivatives of Mie dipole scattering coefficients with respect to the sphere radius, relative permittivity, and permeability of both the sphere and medium. The full theoretical development is presented in Ref. 39.

The Mie dipole scattering coefficients a_1^{sc} and b_1^{sc} are⁴⁰

$$a_1^{\text{sc}} = -\frac{\mu_{r1}\psi_1(m_1x)\psi_1'(m_2x) - \mu_{r2}m\psi_1'(m_1x)\psi_1(m_2x)}{\mu_{r1}\psi_1(m_1x)\xi_1'(m_2x) - \mu_{r2}m\psi_1'(m_1x)\xi_1(m_2x)}, \quad (\text{A1})$$

$$b_1^{\text{sc}} = -\frac{\mu_{r1}\psi_1'(m_1x)\psi_1(m_2x) - \mu_{r2}m\psi_1(m_1x)\psi_1'(m_2x)}{\mu_{r1}\psi_1'(m_1x)\xi_1(m_2x) - \mu_{r2}m\psi_1(m_1x)\xi_1'(m_2x)}, \quad (\text{A2})$$

where $m_1 = \sqrt{\epsilon_{r1}\mu_{r1}}$ and $m_2 = \sqrt{\epsilon_{r2}\mu_{r2}}$ are the real refractive indices of the sphere and medium, respectively, in which ϵ_{ri} and μ_{ri} ($i = 1, 2$) are the real relative permittivity and permeability of the sphere ($i = 1$) and medium ($i = 2$); $m = m_1/m_2$ is the refractive index of the sphere relative to the medium; $x = k_0a = \omega\sqrt{\epsilon_0\mu_0}a$ is the electrical radius of the sphere, given ϵ_0 and μ_0 are the permittivity and permeability of the free space, a is the radius of the sphere; and the prime denotes differentiation with respect to the argument of the function. Note that ϵ_{ri} and μ_{ri} ($i = 1, 2$) defined in this Appendix and the same notations in Sec. II are refer to different physical parameters. Further,

$$\psi_1(z) \equiv zj_1(z) \quad \text{and} \quad \xi_1(z) \equiv zh_1^{(1)}(z), \quad (\text{A3})$$

where $\psi_1(z)$ and $\xi_1(z)$ are Riccati-Bessel functions of order 1 defined in terms of the spherical Bessel function of the first kind of order 1, $j_1(z)$, and the spherical Hankel function of the first kind of order 1, $h_1^{(1)}(z)$ [chap. 4 in Ref. 41].

To obtain the analytical expressions for the derivatives of a_1^{sc} and b_1^{sc} , the following identities are used:^{42,43}

$$\psi_1'(z)\xi_1(z) - \psi_1(z)\xi_1'(z) = -i, \quad (\text{A4})$$

$$\psi_1''(z)\xi_1(z) - \psi_1(z)\xi_1''(z) = 0, \quad (\text{A5})$$

$$\psi_1''(z)\xi_1'(z) - \psi_1'(z)\xi_1''(z) = -i\left(1 - \frac{2}{z^2}\right), \quad (\text{A6})$$

where i is the imaginary unit $\sqrt{-1}$. Note that there should be an extra minus sign on the right hand side of Eqs. (14) and (17) in Ref. 43, which have been remedied in Eqs. (A4) and (A6). Based on these expressions, the Mie derivatives are obtained and shown in Eqs. (A7)–(A16).

$$\frac{\partial a_1}{\partial x} = i \left\{ \frac{\mu_{r2}(\mu_{r2} - \mu_{r1})\frac{m_2^2}{m_1^2}[\psi_1'(m_1x)]^2 + \mu_{r1}\mu_{r2}\frac{m_2^2}{m_1^2}\psi_1(m_1x)\psi_1''(m_1x) + \mu_{r1}^2m_2[\psi_1(m_1x)]^2\left[1 - \frac{2}{(m_2x)^2}\right]}{[\mu_{r1}\psi_1(m_1x)\xi_1'(m_2x) - \mu_{r2}m\psi_1'(m_1x)\xi_1(m_2x)]^2} \right\}, \quad (\text{A7})$$

$$\frac{\partial b_1}{\partial x} = i \left\{ \frac{\mu_{r1}(\mu_{r1}m_2 - \mu_{r2}\frac{m_1^2}{m_2^2})[\psi_1'(m_1x)]^2 + \mu_{r1}\mu_{r2}\frac{m_1^2}{m_2^2}\psi_1(m_1x)\psi_1''(m_1x) + \mu_{r2}^2\frac{m_1^2}{m_2^2}[\psi_1(m_1x)]^2\left[1 - \frac{2}{(m_2x)^2}\right]}{[\mu_{r1}\psi_1'(m_1x)\xi_1(m_2x) - \mu_{r2}m\psi_1(m_1x)\xi_1'(m_2x)]^2} \right\}, \quad (\text{A8})$$

$$\frac{\partial a_1}{\partial \epsilon_{r1}} = 0.5i \left\{ \frac{\mu_{r1}^2\sqrt{\frac{\mu_{r2}}{\epsilon_{r2}}}x\{\psi_1(m_1x)\psi_1''(m_1x) - [\psi_1'(m_1x)]^2\} + \mu_{r1}^{1.5}\sqrt{\frac{\mu_{r2}}{\epsilon_{r1}\epsilon_{r2}}}\psi_1(m_1x)\psi_1'(m_1x)}{[\mu_{r1}\psi_1(m_1x)\xi_1'(m_2x) - \mu_{r2}m\psi_1'(m_1x)\xi_1(m_2x)]^2} \right\}, \quad (\text{A9})$$

$$\frac{\partial b_1}{\partial \epsilon_{r1}} = 0.5i \left\{ \frac{\mu_{r1}^2\sqrt{\frac{\mu_{r2}}{\epsilon_{r2}}}x\{\psi_1(m_1x)\psi_1''(m_1x) - [\psi_1'(m_1x)]^2\} - \mu_{r1}^{1.5}\sqrt{\frac{\mu_{r2}}{\epsilon_{r1}\epsilon_{r2}}}\psi_1(m_1x)\psi_1'(m_1x)}{[\mu_{r1}\psi_1'(m_1x)\xi_1(m_2x) - \mu_{r2}m\psi_1(m_1x)\xi_1'(m_2x)]^2} \right\}, \quad (\text{A10})$$

$$\frac{\partial a_1}{\partial \mu_{r1}} = 0.5i \left\{ \frac{\epsilon_{r1}\mu_{r1}\sqrt{\frac{\mu_{r2}}{\epsilon_{r2}}}x\{\psi_1(m_1x)\psi_1''(m_1x) - [\psi_1'(m_1x)]^2\} - \sqrt{\frac{\epsilon_{r1}\mu_{r1}\mu_{r2}}{\epsilon_{r2}}}\psi_1(m_1x)\psi_1'(m_1x)}{[\mu_{r1}\psi_1(m_1x)\xi_1'(m_2x) - \mu_{r2}m\psi_1'(m_1x)\xi_1(m_2x)]^2} \right\}, \quad (\text{A11})$$

$$\frac{\partial b_1}{\partial \mu_1} = 0.5i \left\{ \frac{\epsilon_{r1} \mu_{r1} \sqrt{\frac{\mu_2}{\epsilon_2}} x \{ \psi_1(m_1 x) \psi_1''(m_1 x) - [\psi_1'(m_1 x)]^2 \} + \sqrt{\frac{\epsilon_{r1} \mu_{r1} \mu_2}{\epsilon_2}} \psi_1(m_1 x) \psi_1'(m_1 x)}{[\mu_{r1} \psi_1'(m_1 x) \xi_1(m_2 x) - \mu_{r2} m \psi_1(m_1 x) \xi_1'(m_2 x)]^2} \right\}, \quad (\text{A12})$$

$$\frac{\partial a_1}{\partial \epsilon_2} = 0.5i \left\{ \frac{\epsilon_{r1} \mu_{r1} \left(\frac{\mu_2}{\epsilon_2} \right)^{1.5} x [\psi_1'(m_1 x)]^2 + \mu_{r1}^2 \sqrt{\frac{\mu_2}{\epsilon_2}} x [\psi_1(m_1 x)]^2 \left[1 - \frac{2}{(m_2 x)^2} \right] - \sqrt{\epsilon_{r1} \mu_{r2}} \left(\frac{\mu_1}{\epsilon_2} \right)^{1.5} \psi_1(m_1 x) \psi_1'(m_1 x)}{[\mu_{r1} \psi_1(m_1 x) \xi_1(m_2 x) - \mu_{r2} m \psi_1'(m_1 x) \xi_1(m_2 x)]^2} \right\}, \quad (\text{A13})$$

$$\frac{\partial b_1}{\partial \epsilon_2} = 0.5i \left\{ \frac{\mu_{r1}^2 \sqrt{\frac{\mu_2}{\epsilon_2}} x [\psi_1'(m_1 x)]^2 + \epsilon_{r1} \mu_{r1} \left(\frac{\mu_2}{\epsilon_2} \right)^{1.5} x [\psi_1(m_1 x)]^2 \left[1 - \frac{2}{(m_2 x)^2} \right] + \sqrt{\epsilon_{r1} \mu_{r2}} \left(\frac{\mu_1}{\epsilon_2} \right)^{1.5} \psi_1(m_1 x) \psi_1'(m_1 x)}{[\mu_{r1} \psi_1'(m_1 x) \xi_1(m_2 x) - \mu_{r2} m \psi_1(m_1 x) \xi_1'(m_2 x)]^2} \right\}, \quad (\text{A14})$$

$$\frac{\partial a_1}{\partial \mu_2} = 0.5i \left\{ \frac{\epsilon_{r1} \mu_{r1} \sqrt{\frac{\mu_2}{\epsilon_2}} x [\psi_1'(m_1 x)]^2 + \mu_{r1}^2 \sqrt{\frac{\epsilon_2}{\mu_2}} x [\psi_1(m_1 x)]^2 \left[1 - \frac{2}{(m_2 x)^2} \right] + \mu_{r1}^{1.5} \sqrt{\frac{\epsilon_{r1}}{\epsilon_2 \mu_2}} \psi_1(m_1 x) \psi_1'(m_1 x)}{[\mu_{r1} \psi_1(m_1 x) \xi_1'(m_2 x) - \mu_{r2} m \psi_1'(m_1 x) \xi_1(m_2 x)]^2} \right\}, \quad (\text{A15})$$

$$\frac{\partial b_1}{\partial \mu_2} = 0.5i \left\{ \frac{\mu_{r1}^2 \sqrt{\frac{\epsilon_2}{\mu_2}} x [\psi_1'(m_1 x)]^2 + \epsilon_{r1} \mu_{r1} \sqrt{\frac{\mu_2}{\epsilon_2}} x [\psi_1(m_1 x)]^2 \left[1 - \frac{2}{(m_2 x)^2} \right] - \mu_{r1}^{1.5} \sqrt{\frac{\epsilon_{r1}}{\epsilon_2 \mu_2}} \psi_1(m_1 x) \psi_1'(m_1 x)}{[\mu_{r1} \psi_1'(m_1 x) \xi_1(m_2 x) - \mu_{r2} m \psi_1(m_1 x) \xi_1'(m_2 x)]^2} \right\}. \quad (\text{A16})$$

In Eqs. (A7)–(A16), the Riccati-Bessel functions and their derivatives are evaluated as follows. Because the Riccati-Bessel functions are solutions of the Riccati differential equation,⁴⁴

$$z^2 w''(z) + [z^2 - n(n+1)] w(z) = 0, \quad (\text{A17})$$

where $n=0, \pm 1, \pm 2, \dots$, the second order derivative of the Riccati-Bessel functions of order 1 can be expressed as [Eq. (38) in Ref. 43]

$$\psi_1''(z) = \psi_1(z) \left(\frac{2}{z^2} - 1 \right). \quad (\text{A18})$$

Note that there should be an extra minus sign on the right hand side of Eq. (38) in Ref. 43, which has been remedied in Eq. (A18).

The first order derivative of Riccati-Bessel functions of order 1 can be expressed utilizing the recurrence relation⁴⁵

$$\psi_1'(z) = \psi_0(z) - \frac{1}{z} \psi_1(z). \quad (\text{A19})$$

In addition, the recurrence relation for the Riccati-Bessel functions of order 1 is

$$\psi_1(z) = \frac{1}{z} \psi_0(z) - \psi_{-1}(z), \quad (\text{A20})$$

where $\psi_{-1}(z) = \cos z$, $\psi_0(z) = \sin z$, $\xi_{-1}(z) = \cos z + i \sin z$, and $\xi_0(z) = \sin z - i \cos z$. Note that Eqs. (A18)–(A20) also hold for $\xi_1(z)$.

¹N. Engheta and R. W. Ziolkowski, *Electromagnetic Metamaterials: Physics and Engineering Explorations* (Wiley, New York, 2006).

²C. M. Soukoulis and M. Wegener, *Nat. Photonics* **5**, 523 (2011).

³C. Holloway, E. Kuester, J. Baker-Jarvis, and P. Kabos, *IEEE Trans. Antennas Propag.* **51**, 2596 (2003).

⁴C.-W. Qiu and L. Gao, *J. Opt. Soc. Am. B* **25**, 1728 (2008).

⁵Q. Zhao, J. Zhou, F. Zhang, and D. Lippens, *Mater. Today* **12**, 60 (2009).

⁶W. Shu and J. Song, *IEEE Trans. Antennas Propag.* **60**, 1496 (2012).

⁷A. Yaghjian, *IEEE Trans. Antennas Propag.* **50**, 1050 (2002).

⁸R. Shore and A. Yaghjian, *Electron. Lett.* **41**, 578 (2005).

⁹R. Shore and A. Yaghjian, *IEICE Trans. Commun.* **E88B**, 2346 (2005).

¹⁰C. R. Simovski and S. A. Tretyakov, *Phys. Rev. B* **75**, 195111 (2007).

¹¹R. A. Shore and A. D. Yaghjian, *Radio Sci.* **42**, RS6S21, doi:10.1029/2007RS003647 (2007).

¹²R. A. Shore and A. D. Yaghjian, *IEICE Trans. Commun.* **E91B**, 1819 (2008).

¹³R. A. Shore and A. D. Yaghjian, *IEEE Trans. Antennas Propag.* **57**, 3077 (2009).

¹⁴X.-X. Liu and A. Alù, *J. Nanophotonics* **5**, 053509 (2011).

¹⁵X.-X. Liu, D. A. Powell, and A. Alù, *Phys. Rev. B* **84**, 235106 (2011).

¹⁶X.-X. Liu and A. Alù, *Metamaterials* **5**, 56 (2011).

¹⁷R. A. Shore and A. D. Yaghjian, *Radio Sci.* **47**, RS2014, doi:10.1029/2011RS004859 (2012).

¹⁸R. A. Shore and A. D. Yaghjian, *Radio Sci.* **47**, RS2015, doi:10.1029/2011RS004860 (2012).

¹⁹N. I. Landy, S. Sajuyigbe, J. J. Mock, D. R. Smith, and W. J. Padilla, *Phys. Rev. Lett.* **100**, 207402 (2008).

²⁰A. Alu and N. Engheta, *Radio Sci.* **43**, RS4S01 (2008).

²¹N. Papasimakis, V. A. Fedotov, Y. H. Fu, D. P. Tsai, and N. I. Zheludev, *Phys. Rev. B* **80**, 041102 (2009).

- ²²S. Savo, N. Papasimakis, and N. I. Zheludev, *Phys. Rev. B* **85**, 121104 (2012).
- ²³I. Vendik, O. Vendik, and M. Odit, *Microwave Opt. Technol. Lett.* **48**, 2553 (2006).
- ²⁴I. B. Vendik, O. G. Vendik, and M. A. Odit, *Phys. Solid State* **51**, 1590 (2009).
- ²⁵K. L. Kumley and E. F. Kuester, "Effect of scatterer size variations on the reflection and transmission properties of a metamaterial," talk at National Radio Science Meeting, Boulder, CO, 2012.
- ²⁶Y. Li and N. Bowler, *IEEE Trans. Antennas Propag.* **60**, 2727 (2012).
- ²⁷Y. Li and R. A. Shore, *IEEE Trans. Antennas Propag.* **59**, 2753 (2011).
- ²⁸A. Sihvola, *Electromagnetic Mixing Formulas and Applications* (The Institution of Engineering and Technology, London, 1999).
- ²⁹S. I. Grossman, *Calculus*, 3rd ed. (Academic, Orlando, 1984).
- ³⁰Y. Li and N. Bowler, *IEEE Antennas Wireless Propag. Lett.* **10**, 1484 (2011).
- ³¹D. Stroud and F. P. Pan, *Phys. Rev. B* **17**, 1602 (1978).
- ³²W. Lamb, D. M. Wood, and N. W. Ashcroft, *AIP Conf. Proc.* **40**, 240 (1978).
- ³³N. Stefanou and A. Modinos, *J. Phys.: Condens. Matter* **3**, 8135 (1991).
- ³⁴M. C. Rechtsman and S. Torquato, *J. Appl. Phys.* **103**, 084901 (2008).
- ³⁵S. G. Johnson and J. D. Joannopoulos, *Opt. Express* **8**, 173 (2001).
- ³⁶I. Vendik, O. Vendik, I. Kolmakov, and M. Odit, *Opto-Electron. Rev.* **14**, 179 (2006).
- ³⁷J. D. Joannopoulos, S. G. Johnson, J. N. Winn, and R. D. Meade, *Photonic Crystals: Molding the Flow of Light*, 2nd ed. (Princeton University Press, Princeton, 2008).
- ³⁸Y. Li and N. Bowler, in *2011 IEEE International Symposium on Antennas and Propagation* (IEEE, 2011), pp. 1494–1497.
- ³⁹Y. Li and N. Bowler, "Computation of Mie derivatives," (unpublished).
- ⁴⁰J. A. Stratton, *Electromagnetic Theory* (McGraw-Hill, New York, 1941).
- ⁴¹C. F. Bohren and D. R. Huffman, *Absorption and Scattering of Light by Small Particles* (Wiley-VCH, Weinheim, 2004).
- ⁴²H. C. van de Hulst, *Light Scattering by Small Particles* (Wiley, New York, 1957).
- ⁴³R. Grainger, J. Lucas, G. Thomas, and G. Ewen, *Appl. Opt.* **43**, 5386 (2004).
- ⁴⁴M. Abramowitz and I. A. Stegun, *Handbook of Mathematical Functions with Formulas, Graphs and Mathematical Tables* (Dover, New York, 1972).
- ⁴⁵B. Verner, *J. Opt. Soc. Am.* **66**, 1424 (1976).